Available online at www.sciencedirect.com
ScienceDirect
Advances in Space Research 41 (2008) 908–913
ADVANCES IN SPACE RESEARCH (a COSPAR publication)
www.elsevier.com/locate/asr

On the motions of RHESSI flare footpoints

W.Q. Gan [a,*], Y.P. Li [a], L.I. Miroshnichenko [b]

[a] Purple Mountain Observatory, Chinese Academy of Sciences, Nanjing 210008, China
[b] N.V. Pushkov Institute IZMIRAN, Troitsk, Moscow Region 142190, Russia

Received 13 October 2006; received in revised form 29 April 2007; accepted 1 May 2007

Abstract

The footpoint motions of flare hard X-ray (HXR) sources are directly related to the reconnection scenario of a solar flare. In this work, we tried to extract the information of footpoint motions for a number of flares observed with RHESSI. We found that the RHESSI flare results of the footpoint motions strongly support the classification proposed from the observations of YOHKOH/HXT. Furthermore, it is found that a flare can consist of two types of footpoint motions. We discussed the connections of the footpoint motions with the two-dimensional reconnection models.

Keywords: Solar flares; X-ray emission; Magnetic reconnection

1. Introduction

The RHESSI observations presented at least five types of HXR sources (Aschwanden, 2006): footpoint source; looptop source; coronal source; coronal loop source; and the albedo halo. For the footpoint source, it is usually in a conjugate form, that is, two footpoints have a similar temporal and nonthermal profile. For the looptop source, named also Masuda source discovered first with Yohkoh (Masuda et al., 1994), it is in nonthermal form and appears at the top or a little above the soft X-ray (SXR) loop. Both the footpoint sources and looptop source constitute a low-lying loop. While for the coronal source (Lin et al., 2003), it is initially in nonthermal form and appears above the looptop source before the impulsive phase, when there is no chromospheric counterparts. Afterward, it may become a thermal or super hot source. The coronal source was explained to be above the X-points of reconnection regions. Another type of source that has been discovered recently is, coronal loop source (Veronig and Brown, 2004) which has a nonthermal emission. Veronig and Brown (2004) explained this source as electron beams suffering interactions with thick-targets in a dense loop. The albedo source is a diffusive HXR source around the footpoint source, resulted from the Compton backscattering of photons (Schmahl and Hurford, 2002).

These X-ray sources have their internal connections and provide an essential constraint to a basic model of solar flares. Although they are spatially consistent with the standard scenario of flare loop structure, further examinations are obviously necessary. Sui et al. (2003, 2004) found a new evidence for magnetic reconnection that the looptop source and the coronal source has oppositely directed temperature gradients, that is, the temperature of the looptop source increases with the altitude whereas the temperature of the coronal source decreases with altitude. This elaborate scenario means that the highest temperatures must be located in the region just between the looptop source and the coronal source, where the magnetic reconnection happens. It was also thought an evidence for the existence of current sheet.

The motion mode of HXR sources is directly related to the magnetic reconnection. In the classic reconnection model (e.g., Priest and Forbes, 2002), the two HXR footpoint sources should apparently move apart as successive field lines are connected at higher altitude, while the

* Corresponding author.
E-mail address: wqgan@pmo.ac.cn (W.Q. Gan).

0273-1177/$30 © 2008 Published by Elsevier Ltd on behalf of COSPAR.
doi:10.1016/j.asr.2007.05.001

X-point of reconnection should move upward. This upward motion could be manifested by the motions of coronal source or looptop source.

Observationally, the upward motion of HXR looptop source or the increase of loop height with time has been known before (e.g., Tsuneta et al., 1992). The RHESSI observations give clear pictures of this kind of motions. The upward motion of HXR looptop source occurs after the peak of the HXR flux. The upward motion, at a speed of 10–20 km s^{-1}, can be correlated with the HXR flux (Sui et al., 2004) or not (Liu et al., 2004). Differing from the theoretical expectation, a downward motion of looptop HXR source during the early impulsive phase was observed by Sui et al. (2003, 2004). For the three flares studied, they found that within 2–4 min of the impulsive phase, the looptop sources in the 6–12 and 12–25 keV images first descended by about 20% with a velocity of about 10 km s^{-1} and then rose. Recently, Li and Gan (2005, 2006) confirmed this shrinkage motion through measuring the radio flaring loop and the TRACE flaring loops. Although more samples are needed, the downward motion of looptop HXR source before the appearance of usual upward motions seems to be a solid fact. Li and Gan (2006) proposed that the 2.5-dimension reconnection model (e.g., Chen et al., 1999) might not be in contradiction with these new observations.

The observations for the motion of coronal HXR source seem to be very limited so far. Sui et al. (2004) described for one flare that the coronal source stayed stationary for several minutes in the early impulsive phase. After the peak of HXR flux, the coronal source moved outward at a speed of 300 km s^{-1}.

For the motions of HXR footpoint source, the observations are not exactly as that predicted by the theoretical reconnection models. The separation of two footpoint HXR sources across the neutral line can either increase or decrease, and the motion can be in parallel or antiparallel along the arcade (Grigis and Benz, 2005 and reference in). Krucker et al. (2003) studied the motion of HXR footpoint sources for the X4.8 flare of 2002 July 23 and found that one footpoint source moves systematically for more than 10 min, but the other does not. The good correlation between the speed of the motion and the HXR flux was thought a strong evidence for the magnetic reconnection model. The difference from the classic scenario of magnetic reconnection was explained as the complexity of magnetic configuration. However, no correlation between the speed of footpoint motion and HXR flux were also observed recently (Grigis and Benz, 2005), suggesting that the HXR light curve is caused by a spatial displacement along the arcade, that is, a disturbance propagates along the arcade, sequentially triggering a reconnection process in successive loops of the arcade. Krucker et al. (2005) further studied for a RHESSI flare the temporal variations of the velocity of the HXR footpoint motions and the photospheric magnetic field strength.

Recently, based on Yohkoh/HXT data Bogachev et al. (2005) classified the footpoint motions into three types. Type I consists of the motions preferentially away from and nearly perpendicular to the neutral line. Type II manifests the motions mainly along the neutral line in antiparallel directions. Type III is similar to Type II but all the HXR sources move in the same direction along the neutral line. The proportion of Type I, II, and III is 13%, 26%, and 35%, respectively. We see that the traditional two-dimensional reconnection model can directly explain only a small number of flares (Type I). Bogachev et al. (2005) showed a carton to demonstrate the motions of Type II, i.e., the magnetic line reconnection happens in a highly sheared magnetic configuration, while the formation of these sheared magnetic structures may result from large-scale photospheric flows like differential rotation or sheared vortex. For the motions of Type III, it was explained as a displacement of the particle acceleration region during a flare.

In this paper, we concentrate on the motions of RHESSI flare footpoints. We try to extract some good RHESSI examples with two footpoints and study how they move during the flares. Then we discuss them with a comparison of the classification proposed based on YOHKOH/HXT observations.

2. RHESSI sample analysis

Table 1 lists the 9 RHESSI flares we have taken as the samples for the study of the footpoint motions. In each of these samples, there appear always two perfect footpoint sources above 50 keV. The simultaneous observations with the EIT/SOHO or TRACE are available for these samples, so that the spatial comparison of the HXR footpoints can be made.

In order to compare with the classification proposed by Bogachev et al. (2005), we define three parameters: d – the distance of the two footpoints (usually in 50–100 keV); $d_{\|}$ – the projected position of the middle point of the line connecting two footpoints, on the best fitted straight line made of all the middle points; Ω – the angle between the line connecting two footpoints and the best fitted straight line made of all the middle points. Physically, the parameters d, $d_{\|}$, and Ω reflect in some degree the separation motion, the parallel motion, and the antiparallel motion of the two footpoints, respectively. With these parameters, the Type I–III footpoint motions can be translated as follows:

Type I: d increases with time, while both $d_{\|}$ and Ω do not greatly change with time;

Type II: Ω changes monotonously (usually decreases); d increases with time or decreases first and then increases; $d_{\|}$ may present an obvious change;

Type III: $d_{\|}$ changes monotonously; both d and Ω may not present an obvious change.

For each flare in Table 1, we made the cleaned RHESSI images in 50–100 keV (or 25–50 keV) using grids 3–6 and a 20 s integrated time. The HXR footpoint source centroids were deduced from 60% contours. Then we measured the parameters d, $d_{\|}$, and Ω. We did not consider the projection correction but measured only the apparent motions.

Table 1
9 RHESSI flares taken as samples for the study of footpoint motions

No.	Date	Start-peak-end time (UT)	Location	Importance
1	2002 July 23	0018–0035–0047	S13E72	X4.8
2	2002 Aug. 3	1859–1907–1911	S16W76	X1.0
3	2002 Nov. 9	1308–1323–1336	S12W29	M4.6
4	2003 May 29	0051–0105–0112	S06W37	X1.2
5	2003 Nov. 3	0943–0955–1019	N08W77	X3.9
6	2005 Jan. 1	0001–0031–0039	N06E34	X1.7
7	2005 Jan. 17	0659–0952–1007	N15W25	X3.8
8	2005 Jan. 19	0803–0822–0840	N15W51	X1.3
9	2005 Jan. 20	0636–0701–0726	N14W61	X7.1

Mostly the time variation of footpoints is not as ideal as that defined by the Type I, II, and III. Therefore, for each flare, we further divided it into several intervals, and we extracted only intervals that show to be regular motions. For some cases, we visually identified different types through checking the movies of footpoint motions, especially to distinguish the Type I from the Type III. Figs. 1–7 present the footpoint motions for the events in Table 1 except No. 1 and 3 which had been studied by Krucker et al. (2003) and Grigis and Benz (2005). In each figure, the left panel shows the temporal evolution of two conjugate footpoints and a small window exhibiting the footpoint sources superimposing on the TRACE or EIT/SOHO image at or close to the flare time, while the right panel shows the lightcurve of 50–100 keV (or 25–50 keV) and the temporal variation of d (dotted line), $d_{\|}$ (dotted line), and Ω. The shadow area means that the footpoint motion is regular and has been extracted to classify into the types. Table 2 summarizes the results.

3. Discussion and conclusions

To accurately determine the two conjugate footpoints is sometimes not so easy. Due to the limited dynamic range (~10) and the finite lifetime of each footpoint source, it is very hard to guarantee that the connecting line of two brightest sources reflects just the two conjugate sources. A wrongly identified pair of conjugate sources would result in irregular motion. To avoid wrong identification of conjugate pairs of footpoint sources, we have used data only from those time segments when the footpoint motions were regular.

From the Table 2, we see that among the 18 pieces of time interval for nine events, three pieces belong to Type I, nine pieces belong to Type II, and six pieces (including two entire events) belong to Type III. These numbers, we think, are essentially comparable to those given by Bogachev et al. (2005), who got 13%, 26%, and 35%, respectively. Complementary to the work of Bogachev et al. (2005), we found that most events present a mixed two types, either in Type II first and then Type III, or Type II first and then Type I, or Type III first and then Type II. An event with all the three types mixed does not appear in our samples. Besides, we notice that either Type II or Type III may appear in the early impulsive phase but Type I does not. The Type I seems to follow Type II.

For the event on 2005 January 19, the footpoints seem to move in a new form: one moves in the direction that is vertical to the trail of the other footpoint. That is, one footpoint moves away from the neutral line (although we have not given explicitly the neutral line), while the other moves along the neutral line. The similar behavior happens also in

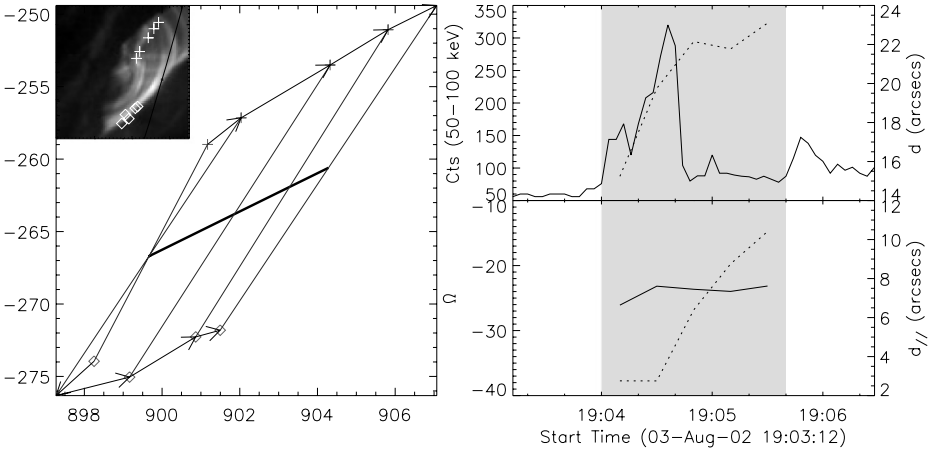

Fig. 1. The two conjugate footpoints variation with time (left panel) and the light curve of 50–100 keV, the temporal variation of d, $d_{\|}$, and Ω (right panel), for the X1.0 flare on 2002 August 3.

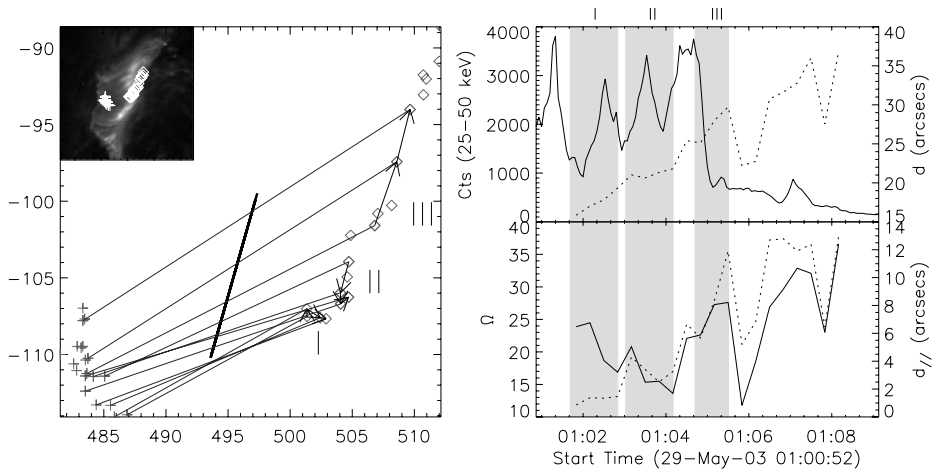

Fig. 2. The same as Fig. 1 but for the X1.2 flare on 2003 May 29.

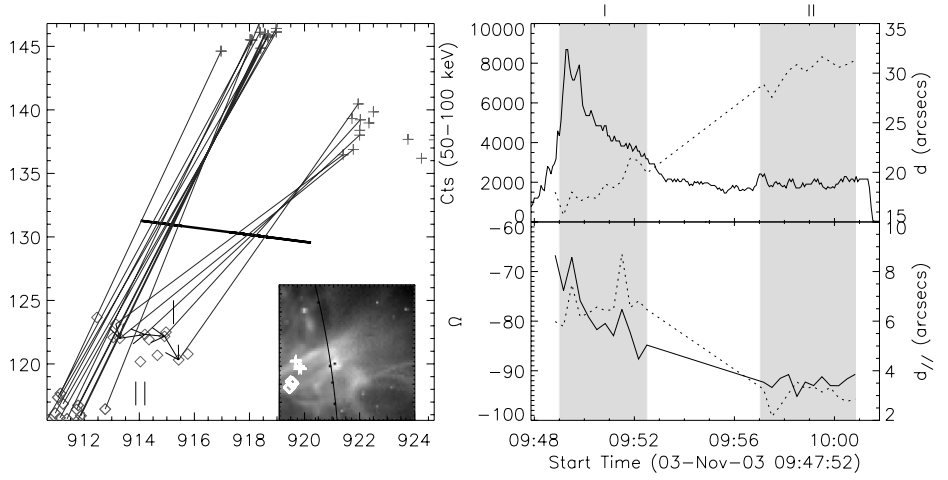

Fig. 3. The same as Fig. 1 but for the X3.9 flare on 2003 November 3.

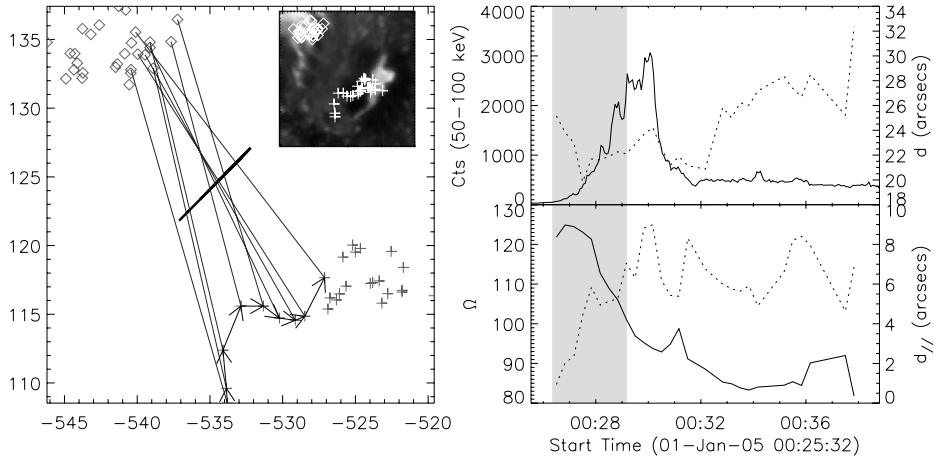

Fig. 4. The same as Fig. 1 but for the X1.7 flare on 2005 January 1.

the event on 2005 January 20 for the time interval II. Although it is not exactly matching to the definition of Type II described above, here we prefer to distribute this kind of motions to a deformed Type II, rather than a new kind of motions. Fig. 8 shows a cartoon to demonstrate how the reconnection for this kind of motions happens. The sheared motion may heavily appear in one side of the neutral line.

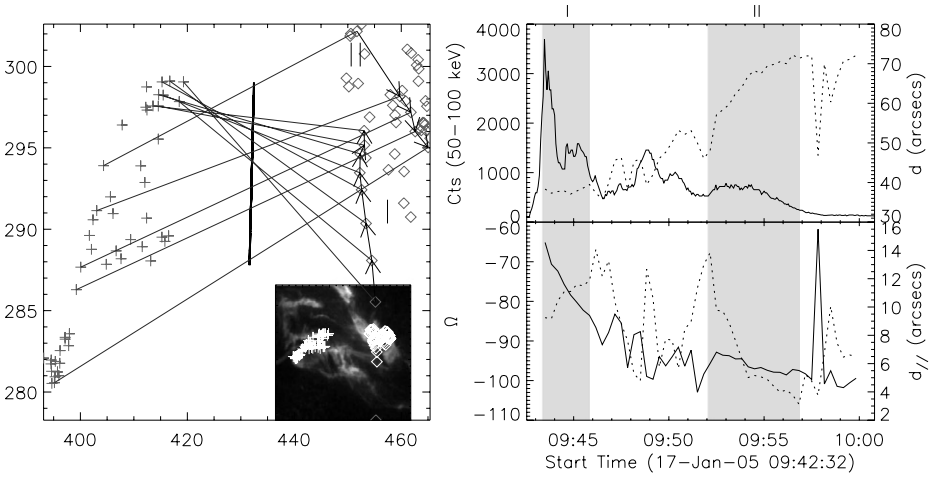

Fig. 5. The same as Fig. 1 but for the X3.8 flare on 2005 January 17.

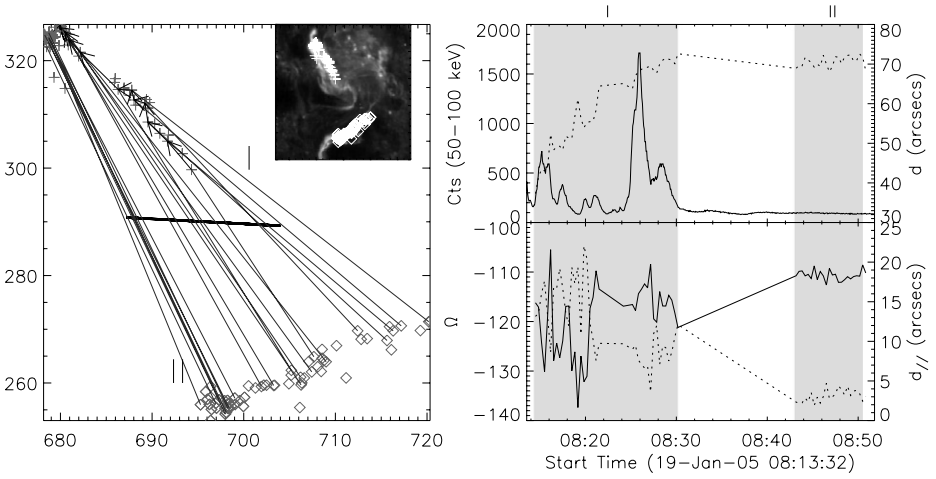

Fig. 6. The same as Fig. 1 but for the X1.3 flare on 2005 January 19.

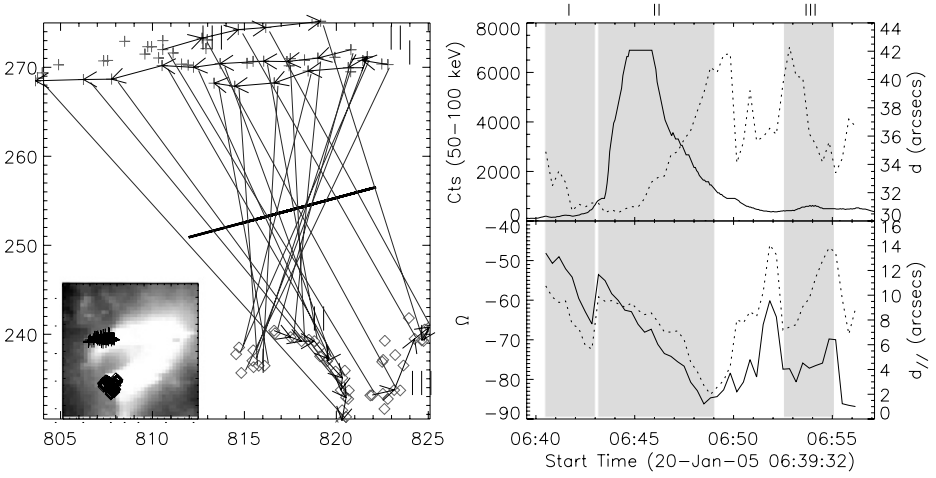

Fig. 7. The same as Fig. 1 but for the X7.1 flare on 2005 January 20.

The standard two-dimensional reconnection model can directly explain the Type I footpoint motions. If the strong sheared motion is taken into account, the Type II footpoint motions can also be understood within the framework of the traditional two-dimensional reconnection model (see also Bogachev et al. (2005)). The Type III of footpoint motions does not seem to be consistent with the two-dimensional reconnection model. It reflects a successive

Table 2
The footpoint motion modes of the 9 RHESSI flares

Flare	Interval 1/Type	Interval 2/Type	Interval 3/Type
1	00:27:40–00:29:40/II	00:35:20–00:39:00/I	
2	19:04:00–19:05:20/III		
3	13:12:10–13:21:30/III		
4	01:01:40–01:02:40/II	01:03:00–01:04:00/II	01:04:40–01:05:20/III
5	09:49:00–09:52:20/II	09:57:00–10:00:40/I	
6	00:26:20–00:27:40/III	00:27:40–00:29:00/II	
7	09:43:20–09:45:40/II	09:52:00–09:56:40/III	
8	08:14:20–08:30:00/II	08:43:00–08:50:20/I	
9	06:40:20–06:42:40/II	06:43:00–06:48:40/II	06:52:20–06:54:40/III

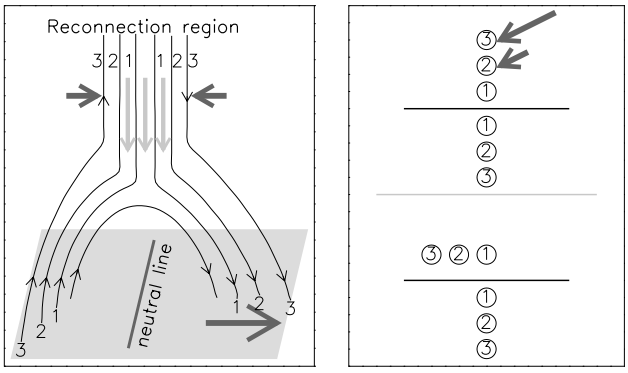

Fig. 8. A sketch demonstrating a deformed Type II footpoint motions.

triggering along the neutral line. Grigis and Benz (2005) proposed a scenario in which a disturbance, probably connected with the eruption of a filament (one of its ends is fixed while the other rises), propagates along the arcade like a burning fuse, sequentially triggering reconnection and particle acceleration in the flare loops. Within this scenario, the main HXR emission from the footpoint reflects the propagation of this disturbance, but not the reconnection process at a given place in the arcade. Obviously, this scenario should be checked in the future. We notice that Tripathi et al. (2006) have identified some "asymmetric eruptive" prominences. To look for corresponding filament eruptions for the event with the Type III footpoint motions is a meaningful work in the future. Anyway, at least at present, we see that the two-dimensional reconnection model works well in explaining the observations of footpoint motions.

In summary, we have analyzed 9 RHESSI flares with two perfect footpoint HXR sources. The results of the footpoint motions strongly support the classifications of Type I, II, and III proposed from YOHKO/HXT observations (Bogachev et al., 2005). It is found that a flare can consist of two types of footpoint motions. The Type III footpoint motions, i.e., the two conjugate footpoints move in parallel along the ribbons, are solidly confirmed. Whether the Type III footpoint motions can be understood within the framework of the two-dimensional reconnection model depends on the future advanced observations; otherwise one needs a new mechanism to explain the successive triggering along the arcade.

Acknowledgements

This work is supported by NNSFC via Grants 10221001, 10333040, 10610099, by NBRPC via Grant 2006CB806302, and by CAS via Grant KJCX2-YW-T04.

References

Aschwanden, M. Physics of the solar corona: an introduction. Springer, Berlin, p. 589, 2006.
Bogachev, S., Somov, B.V., Kosugi, T., Sakao, T. The motions of the hard X-ray sources in solar flares: images and statistics. ApJ 620, 561–572, 2005.
Chen, P.F., Fang, C., Tang, Y.H., et al. Simulation of magnetic reconnection with heat conduction. ApJ 513, 516–523, 1999.
Grigis, P.C., Benz, A.O. The evolution of reconnection along an arcade of magnetic loops. ApJ 625, L143–L146, 2005.
Krucker, S., Hurford, G.J., Lin, R.P. Hard X-ray source motions in the 2002 July 23 gamma-ray flare. ApJ 595, L103–L106, 2003.
Krucker, S., Fivian, M.D., Lin, R.P. Hard X-ray footpoint motions in solar flares: comparing magnetic reconnection models with observations. Adv. Space Res. 35, 1707–1711, 2005.
Li, Y.P., Gan, W.Q. The shrinkage of flare radio loops. ApJ 629, L137–L139, 2005.
Li, Y.P., Gan, W.Q. The oscillatory shrinkage in TRACE 195 Åloops during a flare impulsive phase. ApJ 644, L97–L100, 2006.
Lin, R.P., Krucker, S., Hurford, G.J., et al. RHESSI observations of particle acceleration and energy release in an intense solar gamma-ray line flare. ApJ 595, L69–L72, 2003.
Liu, W., Jiang, Y.W., Liu, S., Petrosian, V. RHESSI observations of a simple large X-ray flare on 2003 November 3. ApJ 611, L53–L56, 2004.
Masuda, S., Kosugi, T., Hara, H., Tsuneta, S., Ogawara, Y. A looptop hard X-ray source in a compact solar flare as evidence for magnetic reconnection. Nature 371, 495–497, 1994.
Priest, E.R., Forbes, T.G. The magnetic nature of solar flares. Astron. Astrophys. Rev. 10, 313–377, 2002.
Schmahl, E.J., Hurford, G.J. RHESSI observations of the size scales of solar hard X-ray sources. Sol. Phys. 210, 273–286, 2002.
Sui, L., Holman, G.D. Evidence for the formation of a large-scale current sheet in a solar flare. ApJ 596, L251–L254, 2003.
Sui, L., Holman, G.D., Dennis, B.R. Evidence for magnetic reconnection in three homologous solar flares observed by RHESSI. ApJ 612, 546–556, 2004.
Tripathi, D., Isobe, H., Mason, H.E. On the propagation of brightening after filament/prominence eruptions, as seen by SOHO–EIT. A&A 453, 1111–1116, 2006.
Tsuneta, S., Hara, H., Shimizu, T., et al. Observation of a solar flare at the limb with the YOHKOH soft X-ray telescope. PASJ 44 (No. 5), L63–L69, 1992.
Veronig, A.M., Brown, J.C. A coronal thick-target interpretation of two hard X-ray loop events. ApJ 6–3, L117–L120, 2004.